

# Antibacterial mechanisms of a novel type picosecond laser-generated silver-titanium nanoparticles and their toxicity to human cells

Peri Korshed<sup>1</sup>  
 Lin Li<sup>2</sup>  
 Zhu Liu<sup>3</sup>  
 Aleksandr Mironov<sup>4</sup>  
 Tao Wang<sup>1</sup>

<sup>1</sup>School of Biological Science, Faculty of Biology, Medicine and Health, <sup>2</sup>Laser Processing Research Centre, School of Mechanical, Aerospace and Civil Engineering, <sup>3</sup>School of Materials, <sup>4</sup>Core Research Facilities, Faculty of Biology, Medicine and Health, The University of Manchester, Manchester, UK

Correspondence: Tao Wang  
 School of Biological Science, Faculty of Biology, Medicine and Health, The University of Manchester, AV Hill Building 1.014, Oxford Road, Manchester M13 9PL, UK  
 Tel +44 161 275 1508  
 Fax +44 161 275 3938  
 Email tao.wang@manchester.ac.uk

Lin Li  
 Laser Processing Research Centre, School of Mechanical, Aerospace and Civil Engineering, The University of Manchester, Manchester M13 9PL, UK  
 Tel +44 161 306 3816  
 Fax +44 161 306 3803  
 Email lin.li@manchester.ac.uk

**Abstract:** In this study, we explored the antibacterial mechanisms for a novel type of Ag-TiO<sub>2</sub> compound nanoparticles (NPs) produced from an Ag-TiO<sub>2</sub> alloy using a picosecond laser and evaluated the toxicity of the Ag-TiO<sub>2</sub> NPs to a range of human cell types. Transmission electron microscopy was used to determine the morphology, shapes, and size distribution of the laser-generated Ag-TiO<sub>2</sub> NPs. UV-visible spectrometer was used to confirm the shift of light absorbance of the NPs toward visible light wavelength. Results showed that the laser-generated Ag-TiO<sub>2</sub> NPs had significant antibacterial activities against both Gram-negative and Gram-positive bacterial strains, including *Escherichia coli*, *Pseudomonas aeruginosa*, and the methicillin-resistant *Staphylococcus aureus*. Increased level of reactive oxygen species was produced by *E. coli* after exposure to the Ag-TiO<sub>2</sub> NPs, which was accompanied with lipid peroxidation, glutathione depletion, disintegration of cell membrane and protein leakage, leading to the cell death. Five types of human cells originated from lung (A549), liver (HePG2), kidney (HEK293), endothelium cells (human coronary artery endothelial cells [hCAECs]), and skin (human dermal fibroblast cells [HDFc]) were used to evaluate the cytotoxicity of the laser-generated Ag-TiO<sub>2</sub> NPs. A weak but statistically significant decrease in cell proliferation was observed for hCAECs, A549 and HDFc cells when co-cultured with 2.5 µg/mL or 20 µg/mL of the laser-generated Ag-TiO<sub>2</sub> NPs for 48 hours. However, this effect was no longer apparent when a higher concentration of NPs (20 µg/mL) was used after 72 hours of co-culture with human cells, suggesting a possible adaptive process in the cells had occurred. We conclude that picosecond laser-generated Ag-TiO<sub>2</sub> NPs have a broad spectrum of antibacterial effect, including against the drug-resistant strain, with multiple underlying molecular mechanisms and low human cell toxicity. The antimicrobial properties of the new type of picoseconds laser-generated Ag-TiO<sub>2</sub> compound NPs could have potential biomedical applications.

**Keywords:** silver-titanium nanoparticles, bactericidal, picoseconds laser, reactive oxygen species, cytotoxicity, compound nanoparticles, methicillin-resistant *Staphylococcus aureus*

## Introduction

Silver nanoparticles (Ag NPs) and titanium oxide nanoparticles (TiO<sub>2</sub> NPs) are the two types of nanoparticles (NPs) that are most widely used as antimicrobial agents. Silver was historically known to have antibacterial properties and has been used against a wide range of bacteria, fungi and viruses.<sup>1</sup> The applications of Ag NPs include, but not limited to, water purification, disinfection of medical devices, treating burns and wounds.<sup>2-4</sup> However, Ag NPs are prone to oxidation that results in loss of antibacterial properties. Ag NPs can also be expensive if large amounts are required. On the other hand, TiO<sub>2</sub> NPs are more stable and cheaper than Ag NPs, but their activation requires

ultraviolet (UV) light illumination to initiate a photocatalyst process, which limits their applications.<sup>5</sup> To maximize the application potential of both Ag NPs and TiO<sub>2</sub> NPs, composite Ag and TiO<sub>2</sub> NPs were produced in recent years.<sup>6,7</sup> Combinations of Ag NPs with TiO<sub>2</sub> NPs could enhance the photocatalytic property of TiO<sub>2</sub> by promoting electron-hole separation and introducing more surface area absorption.<sup>8</sup> Adsorption of visible light by Ag NPs surface could also stimulates electron transfer to TiO<sub>2</sub> NPs, resulting in charge separation and activation of TiO<sub>2</sub> NPs by visible light.<sup>9</sup>

The molecular and cellular mechanisms that underline the antibacterial properties of either Ag NPs or TiO<sub>2</sub> NPs separately have been studied extensively.<sup>10,11</sup> Under UV light, the electron-holes in TiO<sub>2</sub> NPs interact with water and oxygen to generate reactive oxygen species (ROS), especially hydroxyl radicals,<sup>12</sup> achieving antibacterial effects. Multiple mechanisms, including ROS generation contribute to the bactericidal effect of Ag NPs.<sup>10</sup> However, the molecular mechanisms by which the composite Ag-TiO<sub>2</sub> NPs kill bacteria have been largely underinvestigated. In addition, the toxicity of the Ag-TiO<sub>2</sub> composite NPs to human cells are awaiting to be fully characterized. It is known that TiO<sub>2</sub> is relatively safe<sup>13</sup> and has been approved by the US Food and Drug Administration (FDA) to be used as a colorant in food, drugs and cosmetics, including sunscreens.<sup>14</sup> The toxic effect of Ag NPs on human cells, however, is a subject of debate.<sup>15,16</sup> It is believed that the cytotoxicity of Ag NPs to humans is generally low, but numerous reports did show side effects of Ag NPs. For example, long time skin exposure to Ag NPs could turn the skin into bluish gray called argyria.<sup>17</sup> Structure changes in human liver cells were observed when exposing to Ag NPs.<sup>17</sup> The toxic effect of Ag NPs could potentially be reduced when combined with TiO<sub>2</sub> NPs through reducing the amount of Ag NPs used, but there is hardly any information documenting the cytotoxicity of the composite Ag-TiO<sub>2</sub> NPs.

Composite Ag and TiO<sub>2</sub> NPs can be produced in different ways. Majority of them were generated by chemical,<sup>18</sup> sonochemical<sup>19</sup> or sol-gel based methods.<sup>20</sup> Juan et al deposited Ag NPs on titanium surface by salinization. Their results showed that the composite Ag-TiO<sub>2</sub> surface could kill 94% of *Staphylococcus aureus* and 95% of *Escherichia coli* after 24 hours incubation.<sup>4</sup> Using a chemically based method, Pan et al synthesized Ag and TiO<sub>2</sub> nanocomposite, which could completely inhibit *E. coli* survival under visible light irradiation and the antibacterial activity was 5 folds higher than that of TiO<sub>2</sub> alone.<sup>21</sup> Ag-doped TiO<sub>2</sub> NPs were synthesized, which showed antibacterial effects against 3 bacterial strains, *E. coli*, *Pseudomonas aeruginosa* and *S. aureus*

under visible light irradiation and the antibacterial activity of the Ag-doped TiO<sub>2</sub> NPs was superior to TiO<sub>2</sub> NPs alone.<sup>6</sup> However, NPs generated by these methods inevitably carry chemical contaminants. Additional cleaning steps are usually required to purify the NPs, which would complicate the application process.

Recently, we have applied laser technology to the production of NPs.<sup>10,22</sup> The process is carried out in pure water, free of any chemical contaminations. Composite NPs can be rapidly generated by simultaneous ablation of bulk metal blocks in the same reaction using a laser beam. The physical properties of NPs can also be controlled by applying various laser processing parameters.<sup>23</sup> Therefore, the laser-generated NPs have great potential for biomedical applications. Using picosecond laser ablation, we have recently produced Ag-doped TiO<sub>2</sub> NPs from a Ti/Ag bulk alloy for the first time.<sup>22</sup> The Ag-TiO<sub>2</sub> compound NPs significantly shifted the TiO<sub>2</sub> optical absorption spectra to longer visible light wavelength (~500 nm), and initial experiment demonstrated their antibacterial effect against *E. coli* under day light.<sup>22</sup>

In the present study, we conducted a comprehensive characterization on the antibacterial activities of this novel type of laser-generated Ag-TiO<sub>2</sub> NPs against the Gram-negative bacteria *E. coli* and *P. aeruginosa*, and the Gram-positive and methicillin-resistant *S. aureus* (MRSA) under day light condition, explored the molecular mechanisms underlying the antibacterial effects, and evaluated toxicity against 5 types of human cells. We found that the picosecond laser-generated Ag-TiO<sub>2</sub> compound NPs had a broad spectrum of antibacterial effect, including the drug-resistant strain MRSA with low human cell toxicity. Multiple mechanisms, including increased cellular ROS generation, lipid peroxidation (LPO), glutathione (GSH) depletion, disintegration of cell membrane and protein leakage contributed to the bactericidal effects of the laser-generated compound Ag-TiO<sub>2</sub> NPs.

## Materials and methods

### NP production

NPs were produced by pulsed laser ablation of bulk metal blocks in an aqueous phase (deionized water) as described in our previous publications.<sup>22</sup> Ag-TiO<sub>2</sub> NPs were generated by laser ablation of Ag/Ti alloy. For a comparative study, TiO<sub>2</sub> NPs and Ag NPs were generated by laser ablation of Ti plate and Ag plate, respectively. Briefly, the Ag/Ti alloy plate, Ti plate and Ag plate were washed with ethanol and sterile deionized water to remove any organic compounds on the target surfaces. The metal plates were then placed at the bottom of a 70 mL glass vessel that contained 20 mL

of dH<sub>2</sub>O. An Edgewave (Würselen, Germany) picosecond laser was used to produce the NPs with the following parameters: wavelength  $\lambda=1,064$  nm, frequency  $f=200$  kHz, laser power  $P=9.12$  W, pulse width  $t=10$  ps, spot size  $D=125$   $\mu\text{m}$ , scan speed  $v=250$  mm s<sup>-1</sup>, laser pulse energy  $E_{\text{pulse}}=45.6$   $\mu\text{J}$  and laser fluence  $F_{\text{laser}}=0.3717$  J/cm<sup>2</sup>.

## UV-visible spectrophotometry

The absorption spectrum of different concentrations of laser-generated TiO<sub>2</sub> and Ag-TiO<sub>2</sub> NPs was measured by Synergy HTX Multi-Mode Reader (BioTek, Swindon, UK). Quartz cuvette was used and triplicate samples were measured at each laser Ag and Ag-TiO<sub>2</sub> NP concentration. The absorbance curve was made by plotting the wavelength (100–700 nm) versus the absorbance.

## Bacteria culture and the determination of antibacterial activities of NPs

Single colonies of the Gram-negative bacteria, *E. coli* (JM109, Promega, Southampton, UK) or *P. aeruginosa* (ATCC, 9,027)<sup>24</sup>, or the Gram-positive bacteria, *S. aureus* (ATCC, 43,300 methicillin-resistant strain)<sup>25</sup> were inoculated, in 10 mL of autoclaved Muller–Hinton broth media (Sigma-Aldrich, Dorset, UK), respectively, and then incubated at 37°C overnight with shaking at 225 rpm. The culture of bacteria suspension was diluted to give 10<sup>4</sup> cfu/mL ready to be used for the antibacterial experiments below. The antibacterial activity of NPs was determined following the standard Nathan's agar well-diffusion technique. Briefly, the bacterial culture prepared above was spread uniformly on the Muller–Hinton agar plates using sterile cotton swabs and left for 10 minutes for absorption. Then 6 mm wells were made by punching the Muller–Hinton agar plates with a cylinder glass tube. NP sample solution 50  $\mu\text{L}$  at different concentrations was added into each well and was incubated at 37°C for 18 hours. The zones of inhibition (ZOIs) which reflect the susceptibility of microbes to the NPs were then measured<sup>10</sup> and presented as the average value from 2–4 measurements for each well.

## Detection of ROS generation

ROS detection reagents, 2,7-dichlorofluorescein diacetate (DCFH-DA, Sigma-Aldrich), was used in the study. First of all, *E. coli* bacterial cells in a density of 10<sup>4</sup> cfu/mL were incubated with laser-generated Ag-TiO<sub>2</sub> NPs at different concentrations (10, 30 and 50  $\mu\text{g}/\text{mL}$ ) for 5 hours at 37°C in triplicate with shaking at 225 rpm. The bacterial cells were then pelleted by centrifugation at 1,000 rpm for 5–10 minutes.

The bacterial cell pellet was suspended in 1 mL LB broth. DCFH-DA reagent was added to the cell suspension to give a final concentration of 100  $\mu\text{M}$  followed by incubation at 37°C for 30 minutes in dark. Cell suspension 200  $\mu\text{L}$  was transferred to a well of a 96-well plate in triplicate. The fluorescence was measured by a spectrophotometer (LUMIstar® Omega, BMG LABTECH GmbH, Ortenberg, Germany) at an excitation wavelength 485 nm and emission wavelength 528 nm.<sup>26</sup>

## GSH reductase measurement

*E. coli* of 10<sup>4</sup> cfu/mL was incubated with 15  $\mu\text{g}/\text{mL}$  laser-generated Ag-TiO<sub>2</sub> NPs in the shaker for 3–5 hours. H<sub>2</sub>O<sub>2</sub> (4  $\mu\text{g}/\text{mL}$ ) was used as positive control, and equal volume of dH<sub>2</sub>O was used as negative (NP-free) control. Following the treatment of *E. coli* by Ag-TiO<sub>2</sub> NPs, GSH reductase level was measured according to the manufacturer's instruction. Bacterial samples 100  $\mu\text{L}$  treated with Ag-TiO<sub>2</sub> NPs or the controls were mixed with 500  $\mu\text{L}$  oxidized GSH, 100  $\mu\text{L}$  assay buffer, 250  $\mu\text{L}$  of 5,5'-Dithiobis(2-nitrobenzoic acid), and 50  $\mu\text{L}$  nicotinamide adenine dinucleotide phosphate. Each reaction 200  $\mu\text{L}$  was transferred to a well of 96-well plate and read by the Spectrophotometer (Omega) at 450 nm.

## LPO analysis

LPO malondialdehyde (MDA) assay kit (Cat No MAK085/ Sigma-Aldrich) was used to determine MDA that is a by-product of LPO of bacterial cell membrane. Briefly, bacterial culture (10<sup>4</sup> cfu/mL) was treated with laser-generated Ag-TiO<sub>2</sub> NPs in final concentrations of 5, 10, 15 and 20  $\mu\text{g}/\text{mL}$  by incubating at 37°C with shaking for 3 hours. Bacterial suspension 1 mL was homogenized in ice with 300  $\mu\text{L}$  MDA lysis buffer and 3  $\mu\text{L}$  of butylated hydroxytoluene and then centrifuged at 13,000 $\times$  g for 10 minutes to remove insoluble materials. Then 200  $\mu\text{L}$  of the supernatant from each homogenized sample was placed into a microcentrifuge tube and 600  $\mu\text{L}$  of the thiobarbituric acid (TBA) solution was added into each tube. The reaction was incubated at 95°C for 60 minutes in order for the MDA and TBA to form complex, and then cooled down by placing the tubes into ice bath for 10 minutes. Finally, 200  $\mu\text{L}$  of the reaction from each tube was transferred into a well of 96-well plates for absorbance measurement at a wavelength of 532 nm.

## Lactate dehydrogenase (LDH) release assay

*E. coli* at 10<sup>4</sup> cfu/mL were cultured in 96-well plates in 200  $\mu\text{L}$  Muller–Hinton media in triplicate at 37°C overnight. The cells were then treated with 10  $\mu\text{L}$  laser Ag-TiO<sub>2</sub>

NP concentrations (10, 20 and 50  $\mu\text{g}/\text{mL}$ ) or 10  $\mu\text{L}$   $\text{dH}_2\text{O}$  as control and further incubated at 37°C overnight. Lysis buffer 10  $\mu\text{L}$  from the LDH assay kit (Fisher Scientific, Loughborough, UK/Cat No 88954) was then added and mixed by gently tapping and incubated at 37°C for 45 minutes. Cell lysate 50  $\mu\text{L}$  from each sample was then transferred to a new 96-well plate and 50  $\mu\text{L}$  reaction buffer from the kit was added to each well and mixed gently. The plate was then left at room temperature for 30 minutes in dark before 50  $\mu\text{L}$  stop solution was added to each well and mixed by gentle tapping. Finally, OD absorbance was measured at 490 nm using the spectrophotometer (Omega).

### Bradford assay

The Bradford assay using the Coomassie Blue reagent (Thermo Scientific, Chelmsford, MA, USA/Cat No 23200) was to detect proteins present in the bacterial culture medium which reflects protein leakage from bacterial cells. *E. coli* ( $10^4$  cfu/mL) 1 mL was mixed with 100  $\mu\text{L}$  of laser-generated Ag-TiO<sub>2</sub> NPs in final concentration of 5, 10, 15 and 20  $\mu\text{g}/\text{mL}$  and incubated overnight. Bacteria-Ag-TiO<sub>2</sub> NP mix 1 mL was centrifuged at 12,000 rpm for 10 minutes, and 10  $\mu\text{L}$  supernatant from each sample were transferred to 96-well plates. 250  $\mu\text{L}$  of Coomassie Blue reagent was then added to the well and the sample was mixed by shaking the plate for 30 minutes on a micro plate shaker and then further incubated at room temperature for 10 minutes. The absorbance of the sample was measured at 595 nm using the spectrophotometer (Omega). A standard curve of bovine serum albumin was included in each experiment to determine the protein concentration for each sample.

### DNA fragmentation

Ag-TiO<sub>2</sub> NPs or Ag NPs 1 mL at a concentration of 50  $\mu\text{g}/\text{mL}$  was added to 5 mL of *E. coli* culture ( $10^4$  cfu/mL) to give a final concentration of the NPs to be 10  $\mu\text{g}/\text{mL}$ . The bacterial cells were then cultured at 37°C with constant shaking at 225 rpm for 3 hours. The bacterial cells were then pelleted by centrifugation at 8,000 $\times$  g for 5 minutes, and DNA was extracted using the Genomic DNA kit (Cat No BioLine) according to the instructions by the manufacturer. DNA 200 ng was loaded onto 1% agarose gel in Tris-acetate-EDTA (TAE) buffer in triplicate, and electrophoresis was carried out at constant voltage of 100 V for 1.5 hours.

### Cell culture and cytotoxicity assay

Human lung adenocarcinoma cell line (A549, ATCC), human embryonic kidney cell line (HEK293, ATCC)<sup>27</sup> and

human liver cell line (HepG2, ATCC) were cultured in DMEM that were supplemented with 10% fetal bovine serum and 1% of penicillin/streptomycin. Primary human dermal fibroblast cells (HDFc, C0135C, Invitrogen, Inchinnan, UK) were cultured in DMEM/F12 media and primary human coronary artery endothelial cells (hCAECs, PromoCell, Heidelberg, Germany) were cultured in endothelial growth media with supplements (PromoCell)<sup>28</sup> in 75 cm<sup>2</sup> flasks in a 5% CO<sub>2</sub> incubator at 37°C. MTT (MTT [3,-4,5-dimethylthiazol-2-yl]-2,5-diphenyltetrazolium bromide) assay was used to determine the toxicity of the laser-generated Ag-TiO<sub>2</sub> NPs to the 5 types human cells above. The cells were first dissociated from the culture flasks using triple E (Sigma) and then seeded in 96-well plates in a density of 50 cells/well for HEK393, A549 and HDF cells, and 100 cells/well for the HEMC-1 and HepG2 cells. Twelve hours after cell seeding, the culture media was replaced by 100  $\mu\text{L}$  fresh media containing either 2.5 or 25  $\mu\text{g}/\text{mL}$  laser-generated Ag-TiO<sub>2</sub> NPs and incubated at 37°C in the 5% CO<sub>2</sub> incubator for 24, 48 and 72 hours, respectively. A total of 10  $\mu\text{L}$  of 5 mg/mL MTT solution was added to each well and then 90  $\mu\text{L}$  of culture medium was added to the same well to give a final MTT concentration of 10% (v/v). After 4 hours, further culture at 37°C in the 5% CO<sub>2</sub> incubator, 100  $\mu\text{L}$  dimethyl sulfoxide (DMSO, equivalent to the original culture volume) was added, and the plate was incubated for 30 minutes at room temperature with shaking for color development. Finally, the plate was read using a plate reader at an absorbance wavelength of 600 nm. The background absorbance was measured at wavelength of 690 nm.

### Transmission electron microscopy (TEM)

For the imaging of the human cells, laser-generated Ag-TiO<sub>2</sub> NPs were added to the A549 cell culture to give a final concentration 20  $\mu\text{g}/\text{mL}$  and then incubated at 37°C overnight. The cells were fixed with 4% formaldehyde containing 2.5% glutaraldehyde in 0.1 M 4-(2-hydroxyethyl)-1-piperazineethanesulfonic acid (Hepes) buffer (pH 7.2) for 1 hour. Then the cells were treated with 1% osmium tetroxide and 1.5% potassium ferrocyanide in 0.1 M cacodylate buffer (pH 7.2) for 1 hour. The samples were dehydrated in ethanol series infiltrated with TAAB low viscosity resin and polymerized for 24 hours at 60°C. Sections of 70 nm were prepared with Reichert Ultracut ultramicrotome and observed at FEI Tecnai 12 Biotwin microscope at 100 kV accelerating voltage with Gatan Orius SC1000 CCD camera (Gatan, Inc., Pleasanton, CA, USA).

## Statistical analysis

Data in this study were presented as mean  $\pm$  SEM. Each experiment was performed in triplicate. Statistical significance was determined by one-way analysis of variance/Student's *t*-test. *P*-values of  $<0.05$  were considered significantly different.

## Results

### Antibacterial effects of laser-generated Ag-TiO<sub>2</sub> compound NPs

Ag-TiO<sub>2</sub> NPs were generated by the picosecond laser. The average size of the Ag-TiO<sub>2</sub> NPs was 47 nm, ranging (10–200 nm, Figure 1A and B). UV-visible light absorption spectra for the Ag-TiO<sub>2</sub> NPs and the TiO<sub>2</sub> NPs with various concentrations are presented in Figure 1C and D. The results show that compared with the pure TiO<sub>2</sub> NPs (Figure 1D), the Ag-TiO<sub>2</sub> NPs give rise to a band in the visible range that grows and shifts to longer wavelengths with increases in the NP concentration (Figure 1C). The spectral feature can be attributed to the plasmon-resonance absorption of the Ag NPs. The average zeta potential of Ag-TiO<sub>2</sub> NPs at concentration 50  $\mu\text{g/mL}$  and temperature 25°C was  $-29.1 \pm 6.73$ , suggesting reasonable stability of the colloidal dispersions.

Different concentrations of the laser-generated Ag-TiO<sub>2</sub> NPs were incubated with *E. coli*, *P. aeruginosa* and the MRSA at 37°C. After 24 hours, clear ZOIs were observed for all bacterial strains (Figure 1E), suggesting significant bactericidal effects of the laser Ag-TiO<sub>2</sub> NPs against both Gram-negative and Gram-positive bacteria, including the drug-resistant *S. aureus* strain. In contrast, laser-generated TiO<sub>2</sub> NPs alone did not have any antibacterial effect at the same day light condition (Figure 1E). However, the ZOI for Ag-TiO<sub>2</sub> NPs against *S. aureus* was significantly smaller compared with that of *E. coli* and *P. aeruginosa* (Figure 1E and F). The different effect is likely caused by the structural differences between Gram-positive and Gram-negative bacteria.<sup>29</sup> Therefore, the bactericidal activity of laser-generated Ag-TiO<sub>2</sub> NPs depends not only on the concentration of NPs, but also the type of bacteria.

### Effect of ROS generation by laser-generated Ag-TiO<sub>2</sub> compound NPs

*E. coli* was then used as model bacteria for the determination of Ag-TiO<sub>2</sub> NP-induced ROS generation. ROS indicator DCFH-DA used in the experiment measures a wide spectrum of different ROS species, including singlet oxygen,

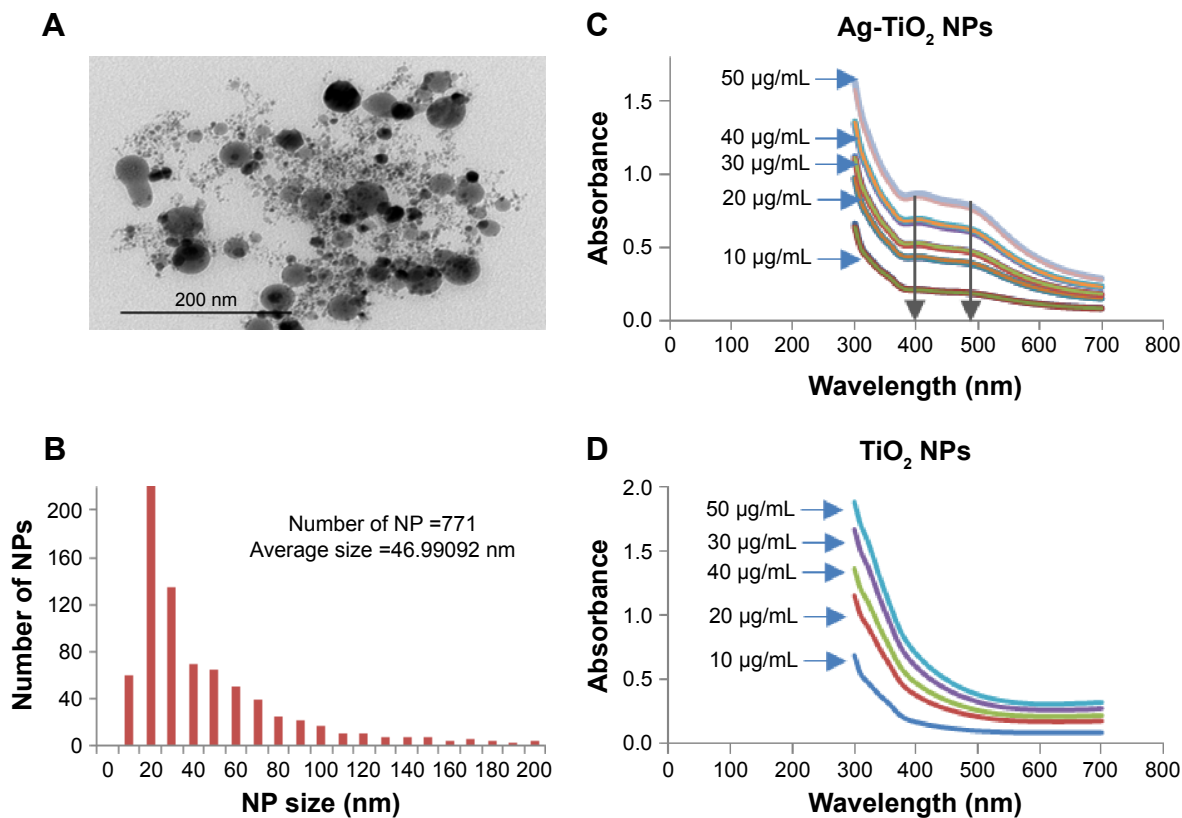
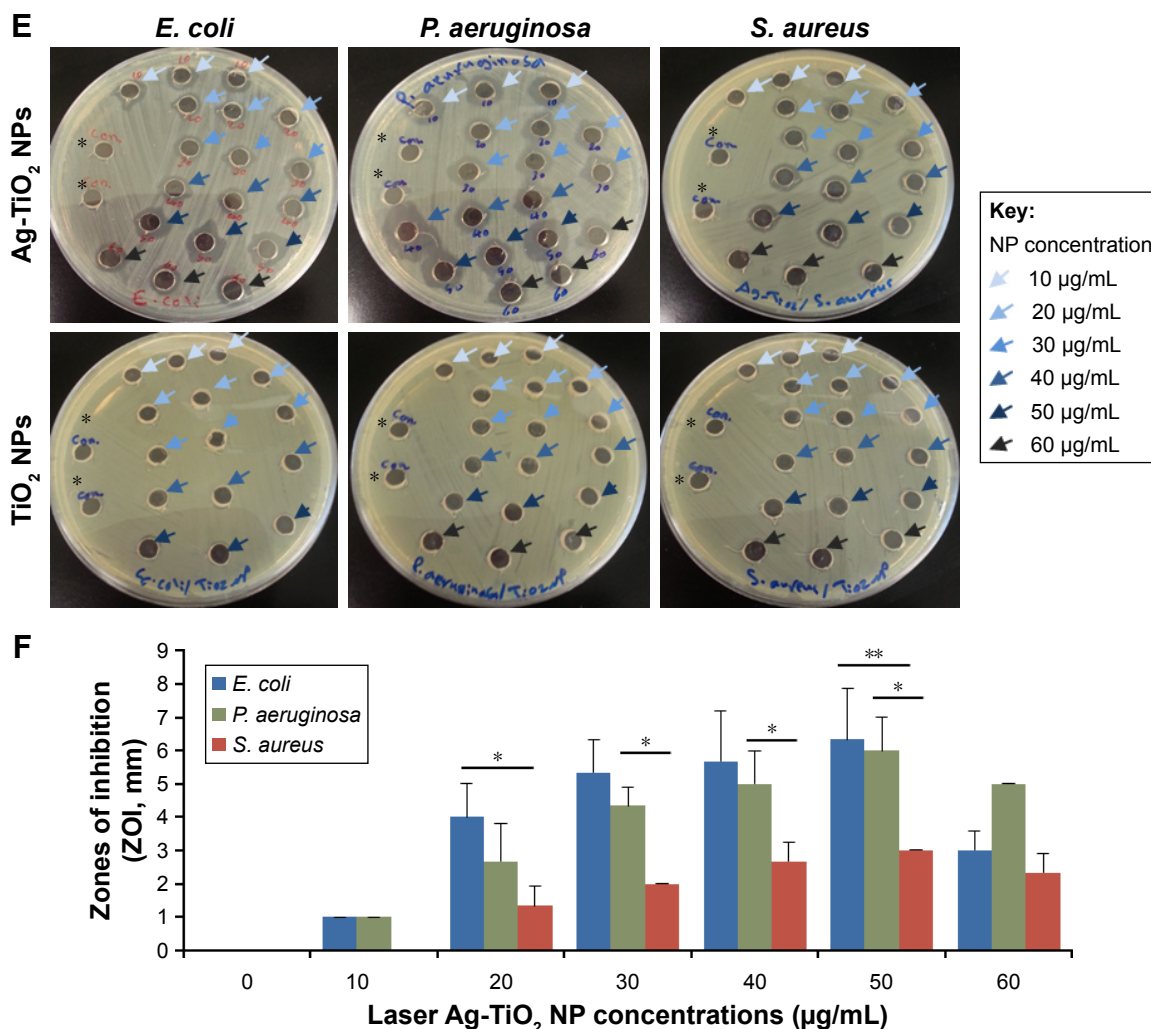


Figure 1 (Continued)



**Figure 1** The antibacterial activity of laser-generated Ag-TiO<sub>2</sub> NPs against Gram-positive and Gram-negative bacteria. **Notes:** TEM image of laser Ag-TiO<sub>2</sub> NPs (A). Size distribution of laser Ag-TiO<sub>2</sub> NPs (B). UV-vis spectrum of Ag-TiO<sub>2</sub> NPs (C) and TiO<sub>2</sub> NPs (D). A lawn of *Escherichia coli*, *Staphylococcus aureus* and *Pseudomonas aeruginosa* were made on Muller–Hinton agar plates and then 6 mm wells were created through the agar. Ag-TiO<sub>2</sub> NPs 50 µL at different concentrations (0, 10, 20, 30, 40, 50 and 60 µg/mL) were added into each well in triplicate for each concentration, and the plates were incubated at 37°C for 24 hours. ZOI (E) was measured and the readings were corrected by the diameter of the well (F). Data are presented as mean ± SE. Compared to *S. aureus* at the same concentration of Ag NPs, \*P≤0.05, \*\*P≤0.01; n=3. **Abbreviations:** NP, nanoparticle; TEM, transmission electron microscopy; ZOI, zone of inhibition.

super oxide, and hydrogen peroxide in addition to hydroxyl radicals. Result showed that the laser-generated Ag-TiO<sub>2</sub> NPs at concentrations of 30 and 50 µg/mL have induced highly significant ROS generation compared with the non-NP treated control samples (Figure 2), suggesting the Ag-TiO<sub>2</sub> NPs induced significant oxidative stress to the bacterial cells.

### Effect of laser-generated Ag-TiO<sub>2</sub> compound NPs on cellular GSH reductase level

To further determine the molecular mechanisms that contribute to the bactericidal effect by the laser-generated Ag-TiO<sub>2</sub> NPs, levels of GSH in *E. coli* was measured after the bacteria were exposed to the laser-generated Ag-TiO<sub>2</sub>

NPs (15 µg/mL) for 3 hours. Results showed that the GSH reductase level was significantly reduced compared with the non-NP treated control samples (Figure 3), suggesting cellular depletion of GSH, a critical antioxidant preventing cellular damages by oxidative stress, has happened in the laser Ag-TiO<sub>2</sub> NPs treated *E. coli*.

### Effect of laser-generated Ag-TiO<sub>2</sub> compound NPs on LPO

ROS accumulation usually leads to LPO, a key mechanism responsible for the increase in cell membrane permeability that contributes to cell death. LPO can be monitored by the generation of malonaldehyde (MAD). Figure 4 shows that the MAD level was significantly increased in the *E. coli*

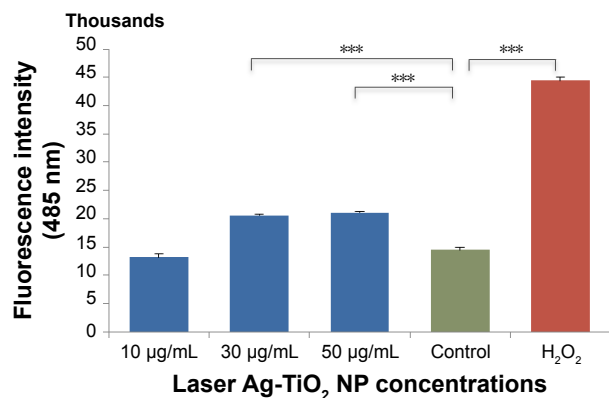


**Figure 2** The effect of laser-generated Ag-TiO<sub>2</sub> NPs on the production of ROS in *Escherichia coli*.

**Notes:** Different concentrations of laser Ag-TiO<sub>2</sub> NPs (10, 30 and 50 µg/mL) were cultured with *E. coli* for 5 hours in triplicate. The ROS levels were measured using the DCFH-DA kit and presented as the fluorescence intensity. Data are mean ± SE. Compared to the NP-free control, \*\*\**P*≤0.001, *n*=3.

**Abbreviations:** DCFH-DA, dichlorofluorescein diacetate; NP, nanoparticle; ROS, reactive oxygen species.

after exposure to the laser Ag-TiO<sub>2</sub> NPs at concentrations of 15 and 20 µg/mL.

## Impact of laser-generated Ag-TiO<sub>2</sub> compound NPs on the integrity of bacterial cell membrane

LDH release is considered to be a reliable indicator of cell membrane damages and increase in permeability. When *E. coli* were exposed to 10 µg/mL laser Ag-TiO<sub>2</sub> NPs for 24 hours, we detected significant LDH increase in the culture media (Figure 5A), suggesting cell membrane damage had occurred. The loss of cell integrity was also demonstrated using the protein leakage analysis. After treating *E. coli* bacterial culture with different concentrations of laser Ag-TiO<sub>2</sub>

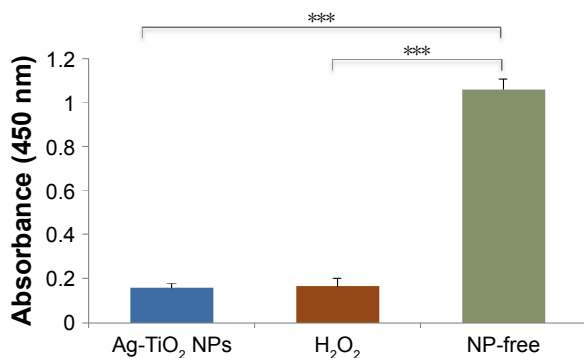


**Figure 3** Changes of cellular glutathione reductase level in laser Ag-TiO<sub>2</sub> NP-treated *Escherichia coli*.

**Notes:** *E. coli* were treated with laser Ag-TiO<sub>2</sub> NPs (15 µg/mL) for 3 hours. The cellular glutathione reductase level was measured using the glutathione assay kit (Sigma). H<sub>2</sub>O<sub>2</sub> (4 µg/mL) treatment was used as a positive control, and the NP-free dH<sub>2</sub>O as a negative control. Data are presented as mean ± SE. Compared to the NP-free control, \*\*\**P*≤0.001, *n*=3.

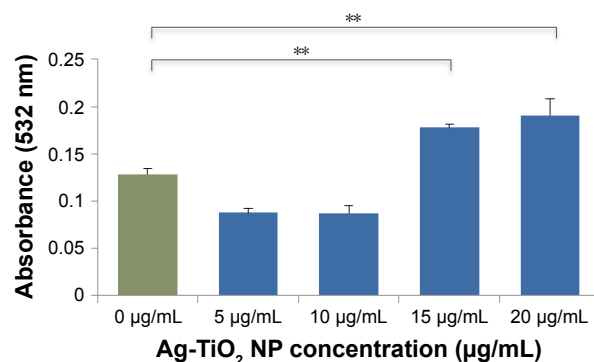


**Figure 4** Lipid peroxidation in *Escherichia coli* by laser-generated Ag-TiO<sub>2</sub> NPs.

**Notes:** Bacterial cells were treated with different concentrations of laser Ag-TiO<sub>2</sub> NPs for 3 hours. Cellular level of malondialdehyde was then measured using the MDA assay Kit (Sigma-Aldrich). Data are presented as mean ± SE. Compared to the NP-free control, \*\**P*≤0.01, *n*=3.

**Abbreviations:** MDA, malondialdehyde; NP, nanoparticle.

NPs (5, 10, 15 and 20 µg/mL) for 24 hours, a dose-dependent increase in the protein level was detected in the culture media as compared with the NP-free control samples (Figure 5B), indicating an increased cell membrane permeability.

## Effect of laser-generated Ag-TiO<sub>2</sub> compound NPs on bacterial DNA damage

The effect of laser Ag-TiO<sub>2</sub> NPs on *E. coli* DNA damage was tested and visualized using DNA agarose gel electrophoresis with the same amount of DNA (200 ng/lane) loaded into each lane. DNA samples treated with Ag-TiO<sub>2</sub> NPs showed no significant change in the major genomic DNA band intensity compared with that of the non-NP treated controls (Figure 6), suggesting Ag-TiO<sub>2</sub> NPs did not induce significant DNA degradation. In contrast, DNA samples treated with the laser-generated Ag NPs had significant reduction of the major DNA band on agarose gel (Figure 6), suggesting significant DNA degradation. Results imply that, compared with Ag NPs, the laser-generated Ag-TiO<sub>2</sub> NPs are less likely causing bacterial DNA damage, and the antibacterial effect of Ag-TiO<sub>2</sub> composite NPs may rely more on the other molecular mechanisms as specified above.

## The toxicity of laser-generated Ag-TiO<sub>2</sub> compound NPs to human cells

To evaluate the potential toxicity of the laser-generated Ag-TiO<sub>2</sub> NPs to humans, 5 types of different human cells originated from the lung (A549 line), the blood vessel (hCAECs), the kidney (HEK293 line), the skin (HDFc cells) and the liver cells (HepG2 line) were tested.<sup>10</sup> The cells were exposed to the laser Ag-TiO<sub>2</sub> NPs for 3 different time

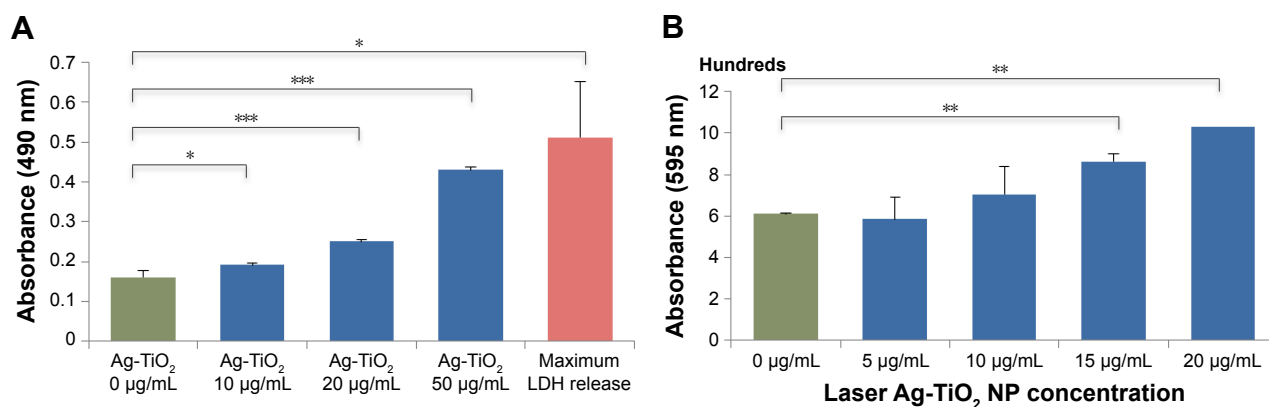


**Figure 5** Effect of laser-generated Ag-TiO<sub>2</sub> NPs on *Escherichia coli* membrane integrity.

**Notes:** *E. coli* were treated with different concentrations of laser Ag-TiO<sub>2</sub> NPs for 24 hours. The culture media were subject for cell membrane integrity analysis using either the LDH assay kit (A) or the Coomassie reagent (B). A positive control was used for the LDH method by freezing and thawing the *E. coli* culture to physically break up the cell membrane integrity, named as maximum LDH release (A). Data are mean ± SE. Compared to the NP-free control, \**P* ≤ 0.05, \*\**P* ≤ 0.01 and \*\*\**P* ≤ 0.001; *n* = 3.

**Abbreviations:** LDH, lactate dehydrogenase; NP, nanoparticle.

periods (24, 48 and 72 hours) at both a low (2.5 µg/mL) and relatively high (20 µg/mL) NP concentrations followed by the MTT assay to measure the viable cells that inversely correlated with the number of dead cells. Slight but statistically significant growth delay was detected for hCAECs after 48 and 72 hours exposure to low concentrations of NPs, but no significant toxicity was observed when 20 µg/mL Ag-TiO<sub>2</sub> NPs were used (Figure 7A). Mild growth delay was also observed for A594 cell after 48 hours NP exposure, but disappeared after further culture up to 72 hours (Figure 7A). Similar mild growth delay was observed for HDFc cells at 48-hour time point when exposed to 20 µg/mL Ag-TiO<sub>2</sub> NPs but returned to normal at 72 hours (Figure 7A). There was no significant cytotoxicity observed for all 5 types of cells after 72 hours exposure to 20 µg/mL Ag-TiO<sub>2</sub> NPs, suggesting an adaptive process had occurred in the cells over time and a low human cell cytotoxicity overall for the laser-generated

Ag-TiO<sub>2</sub> NPs during the testing period. The reliability of the cytotoxicity assay was verified by using hydrogen peroxide (H<sub>2</sub>O<sub>2</sub>) as a cytotoxicity inducer (positive control) on HDFc and A594 cells, which demonstrated that the toxicity of H<sub>2</sub>O<sub>2</sub> to cells could be readily detected by the MTT assay employed in the study (Figure 7B).

To gain further insight into the impact of the laser-generated Ag-TiO<sub>2</sub> NPs to human cells, A594 cells were co-cultured with Ag-TiO<sub>2</sub> NPs (20 µg/mL) for 24 hours, and then imaged by TEM. We observed that the NPs were mainly located outside cell plasma membrane (Figure 8A). Intracellular NPs could be seen but they were rare (Figure 8B). Structure of mitochondrial and other cellular organelles were nicely preserved in the Ag-TiO<sub>2</sub> NP treated cells (Figure 8A and B). Results suggest that Ag-TiO<sub>2</sub> NPs could be relatively non-toxic to mammalian cells. We did not observe any NPs in the cell nuclei, suggesting a low DNA toxicity to human cells.

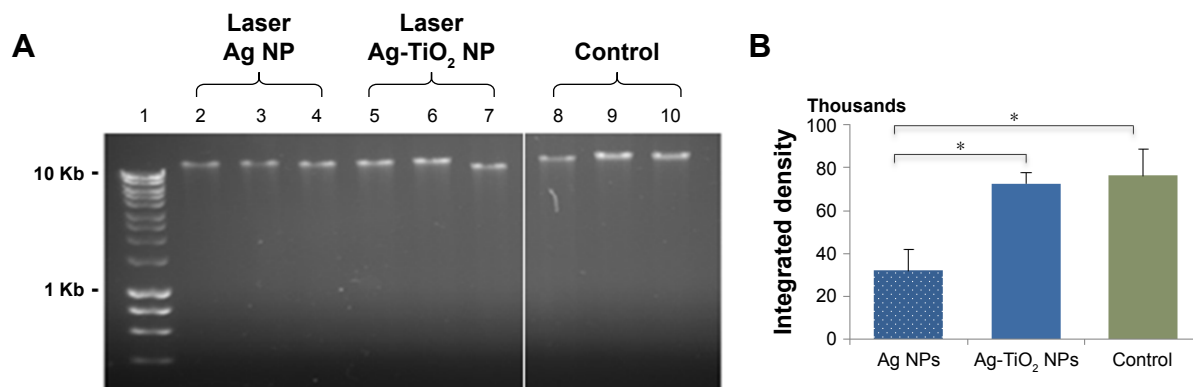


**Figure 6** DNA degradation by laser Ag-TiO<sub>2</sub> NPs in *Escherichia coli*.

**Notes:** *E. coli* were treated by laser-generated Ag-TiO<sub>2</sub> NPs (10 µg/mL) or laser Ag NPs (10 µg/mL) overnight. Genomic DNA were extracted and 200 ng DNA were subjected to agarose gel electrophoresis (A). The intensity of the major DNA bands were quantified and shown in (B). Lane 1, Hyperladder I (BioLine); Lane 5–7, laser Ag-TiO<sub>2</sub> NPs; Lane 2–4, laser Ag NPs; Lane 8–10, NP-free Control. Data were presented as mean ± SE. Compared to the NP-free control, \**P* ≤ 0.05, *n* = 3.

**Abbreviation:** NP, nanoparticle.

## Discussion

In this study, we demonstrated the antibacterial activities of a new type of Ag-TiO<sub>2</sub> compound NPs produced by picosecond laser and explored the molecular mechanisms underlying

the bactericidal effects. The laser-generated Ag-TiO<sub>2</sub> compound NPs had wide spectrum of antibacterial activities against both Gram-negative (*E. coli* and *P. aeruginosa*) and Gram-positive (*S. aureus*) bacteria. To our knowledge,

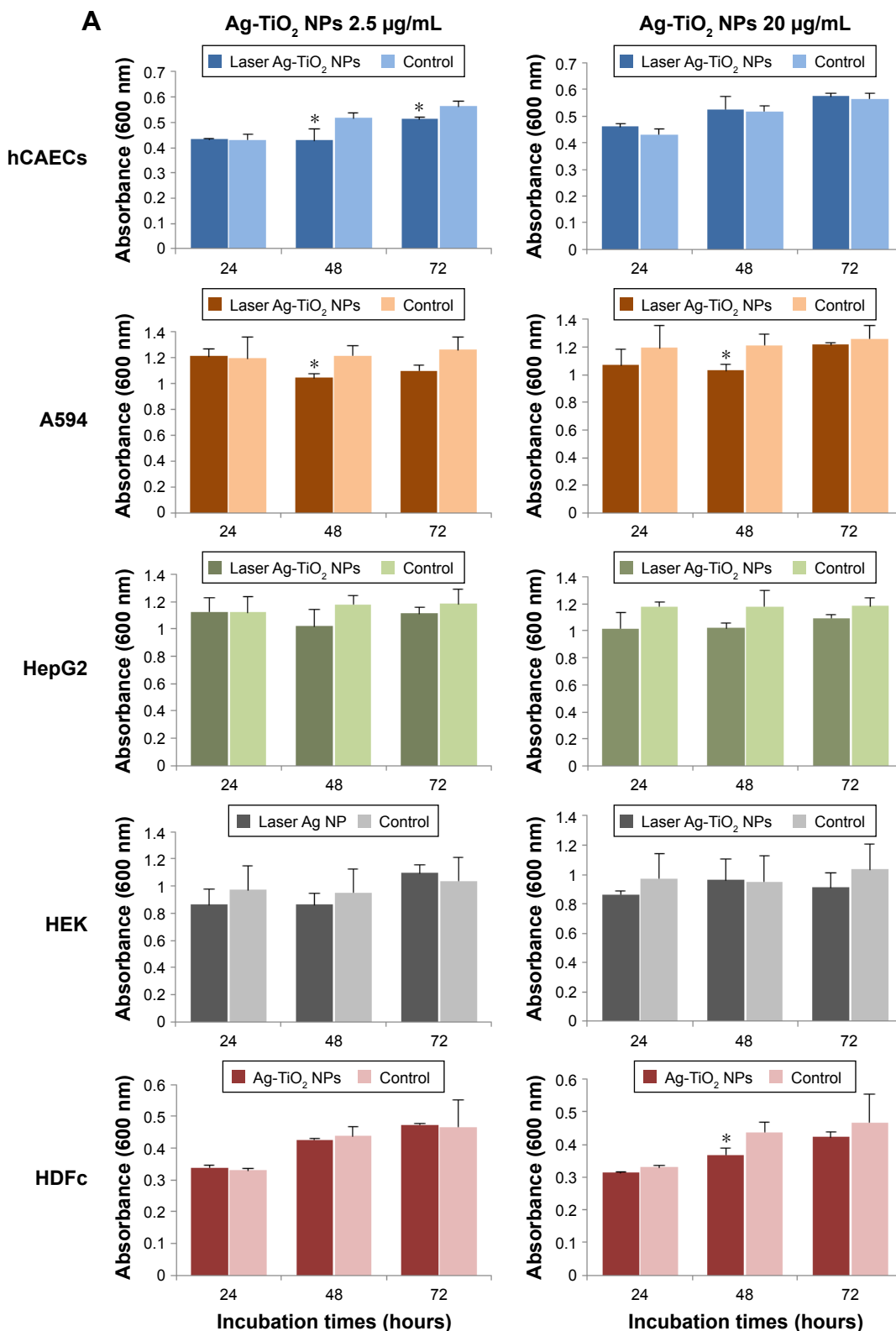
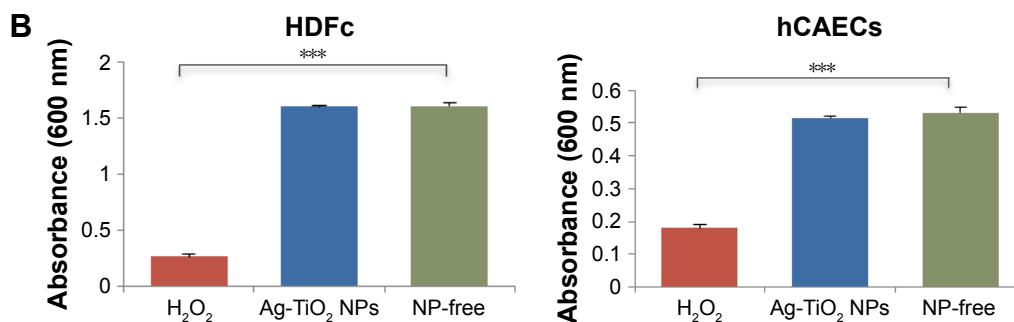


Figure 7 (Continued)



**Figure 7** Cytotoxicity of laser-generated Ag-TiO<sub>2</sub> NPs to human cells.

**Notes:** (A) The laser-generated Ag-TiO<sub>2</sub> NPs at two concentrations (2.5 and 20 µg/mL) were incubated with 5 types of human cells or cell lines: A549 (lung), hCAECs (blood vessel), HEK293 (kidney), HDFc (skin) and the HepG2 (liver), for 24, 48 and 72 hours. Cytotoxicity was determined using MTT assay. (B) H<sub>2</sub>O<sub>2</sub> was used as a positive control. HDFc and hCAECs were treated with either 40 µg/mL H<sub>2</sub>O<sub>2</sub> or with 20 µg/mL Ag-TiO<sub>2</sub> NPs for 24 hours. Toxicity to the cells were measured using MTT assay. Data were presented as mean ± SE. Compared to the NP-free control, \**P*≤0.05, \*\*\**P*≤0.001, *n*=3.

**Abbreviations:** hCAECs, human coronary artery endothelium cells; HDFc, human dermal fibroblast cells; NP, nanoparticle.

there has not been any report on the antibacterial effect of picosecond laser-generated Ag-TiO<sub>2</sub> compound NPs against both Gram-negative and Gram-positive bacterial strains. The *S. aureus* used in the study is a methicillin-resistant strain (MRSA). Our results therefore suggested an application potential for the laser-generated Ag-TiO<sub>2</sub> NPs in medical healthcare for combating drug-resistant microbial infection or contaminations. The Ag-TiO<sub>2</sub> NPs used in our study was directly produced by laser ablation of Ag-TiO<sub>2</sub> NPs alloy in pure water, which provides a green method for rapid production of Ag-TiO<sub>2</sub> composite NPs that could be readily used for health care applications without the need of eliminating contaminants that could be carried over from chemical reactions.

The antibacterial effects of the laser-generated Ag-TiO<sub>2</sub> NPs displayed significant dose dependency within the concentration range from 10 to 50 µg/mL Ag-TiO<sub>2</sub> NPs (Figure 1E and F). At higher concentrations, there would be more NPs in direct contact and interacting with bacterial

cell membrane, leading to better bactericidal effect. We also observed higher susceptibilities of *E. coli* and *P. aeruginosa* to the laser Ag-TiO<sub>2</sub> NPs compared with that of *S. aureus*, (Figure 1E and F). This may be explained by the structural differences between Gram-positive and Gram-negative bacteria where the peptidoglycan layer is thicker in former that serves as a protective layer against chemicals, toxins, derivative enzymes and antibiotics.<sup>29</sup>

Being an antibacterial agent, TiO<sub>2</sub> has several desirable properties, including stability, low toxicity and low cost.<sup>30</sup> The antibacterial effect of TiO<sub>2</sub> NPs attributes to the photocatalytic prosperity of TiO<sub>2</sub>, leading to ROS generation when illuminated by UV light. The requirement for the UV illumination has limited wider applications of TiO<sub>2</sub> NPs, especially when live cells are involved.<sup>31</sup> To overcome this limitation, efforts have been made to load noble metals such as Ag NPs<sup>32</sup> or gold Au NPs<sup>33</sup> onto TiO<sub>2</sub> NPs. Noble metals could enhance the photocatalytic activity of TiO<sub>2</sub> by decreasing band gap of TiO<sub>2</sub> to visible light wave

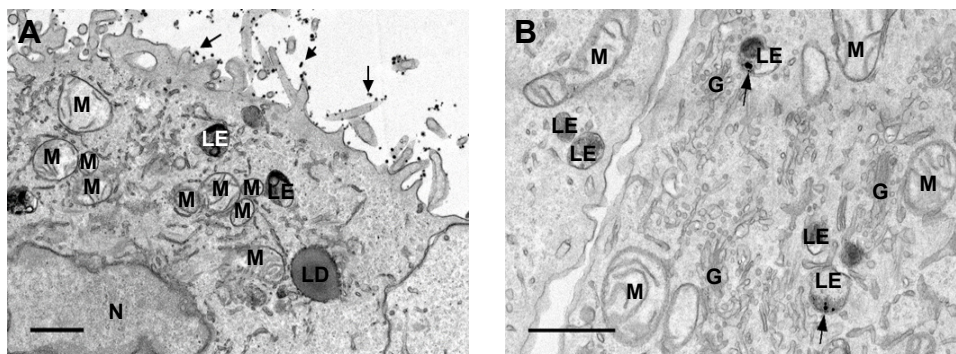


**Figure 8** TEM images of human lung A549 cell line treated with laser-generated Ag-TiO<sub>2</sub> NPs.

**Notes:** TEM imaging was conducted on A549 cells that were treated with laser-generated Ag-TiO<sub>2</sub> NPs (20 µg/mL) for 24 hours. Arrows in (A) indicate extracellular Ag-TiO<sub>2</sub> NPs. Arrows in (B) indicate intracellular Ag-TiO<sub>2</sub> NPs within late endosomes. Scale bars indicate 1 µm.

**Abbreviations:** G, golgi; LD, lipid droplet; LE, late endosomes; M, mitochondria; N, nucleus; NP, nanoparticle; TEM, transmission electron microscopy.

range.<sup>34,35</sup> This feature of TiO<sub>2</sub> was indeed reflected by the laser-generated novel compound Ag-TiO<sub>2</sub> NPs used in this study. The red shift of the absorption curve for the laser Ag-TiO<sub>2</sub> NPs results in the reduction of the band gap energy and also the recombination rate, and hence, enhanced photocatalytic and antibacterial activities from the TiO<sub>2</sub> NPs. The Ag component in the Ag-TiO<sub>2</sub> NPs stores electrons, causing accumulation of so-called Valence-band hole on the TiO<sub>2</sub> NPs, which could initiate oxidation reaction and ROS generation in the absence of light illumination.<sup>36</sup> A study by Cao et al revealed an antibacterial effect of the Ag-TiO<sub>2</sub> NPs in the dark, which was explained by the ability of Ag NPs to trap electrons, thus enhancing the attraction to bacterial cell membranes and leading to cell death.<sup>36</sup>

ROS is considered to be an important mechanism contributing to the antibacterial effect of TiO<sub>2</sub>. We have previously demonstrated an increased ROS generated in the bacterial culture by Ag NPs that were generated by picosecond laser.<sup>10</sup> In the current study, we measured ROS generation by the compound Ag-TiO<sub>2</sub> NPs generated picosecond laser and confirmed that the new type of compound NPs possess the ability of producing ROS in bacteria as their individual composite does. ROS activates cellular antioxidant defense system in order to maintain equilibrium in the redox system. GSH reductase catalyzes the formation of GSH, which is a critical antioxidant to prevent cellular damages by oxidative stress. The excess accumulation of ROS would eventually deplete the cellular GSH pool, leading to insufficient antioxidant to overcome the accumulated ROS, resulting in cell damages.<sup>37</sup> We found that the laser-generated Ag-TiO<sub>2</sub> NPs caused a highly significant reduction of GSH (Figure 3), suggesting the existence of GSH depletion, which contributes the antibacterial effects of the laser Ag-TiO<sub>2</sub> NPs.

ROS generated locally could result in damage of bacterial cell wall and membrane, and increase cell permeability, first to small molecules and then to large molecules such as β-D-galactosidase.<sup>38</sup> Indeed, we detected significant amount of LDH enzyme and other proteins that leaked out of the *E. coli* after incubating with the Ag-TiO<sub>2</sub> NPs (Figure 5A and B). Polyunsaturated phospholipids are the main components of the bacterial cell membrane. MDA is highly reactive byproduct of lipid oxidation that has the ability to react with proteins, forming protein-MDA complex, which is considered as a mutagenic compound. Our results showed that *E. coli* exposed to laser Ag-TiO<sub>2</sub> NPs has increased the production of MDA (Figure 4), which is another mechanisms contributing to the disintegration of the bacteria cell membrane.

Accumulation of intracellular ROS could result in DNA damage. Interestingly, we did not observe significant DNA degradation in *E. coli* that co-cultured with the laser-generated Ag-TiO<sub>2</sub> NPs (Figure 6A and B). This is in contrast with our previous finding on DNA degradation induced by laser-generated Ag NPs.<sup>10</sup> It is likely that mechanisms other than DNA damage could be more important for the bactericidal effects of laser-generated composite Ag-TiO<sub>2</sub> NPs, but additional studies are required to gain further insight.

Endothelial cells are important barriers in the blood vessels of human body that protect blood vessel injury and vascular function. Injury to endothelial cells lead to different pathophysiological disease such as atherosclerosis, myocardial infarction and thrombosis.<sup>39</sup> Mild toxic effect of the laser Ag-TiO<sub>2</sub> NPs was observed at 48 and 72 hours after the endothelial cells had received low concentration (2.5 μg/mL) of the Ag-TiO<sub>2</sub> NPs challenge (Figure 7A). However, the lack of toxicity to endothelial cells at high concentration (20 μg/mL) could be due to the uptake saturation of the NPs and an adaptive response by the cells after 72 hours' co-culture.<sup>41</sup>

The most common route of human exposure to NPs is the respiratory tract, especially when the NPs size is small. After the NPs enter the human body, it will easily reach the alveolar where they either cause local damage to the lung epithelial cells or further travel to spleen, bone marrow and the heart via the blood or lymphatic circulation system for the smaller sized NPs.<sup>41</sup> In this study, we observed that the growth of the A549 cell line that originated from the lung was sensitive to the laser Ag-TiO<sub>2</sub> NPs treatment for 48 hours at both low (2.5 μg/mL) and high (20 μg/mL) concentrations of laser Ag-TiO<sub>2</sub> NPs (Figure 7A). However, similar to what we have observed on the endothelial cells and skin fibroblast, the toxic effects were no longer obvious when the NPs were further incubated with the cells for up to 72 hours (Figure 7A), possibly through a similar adaptive mechanism as mentioned above for the endothelial.<sup>40</sup>

TEM images showed that the laser Ag-TiO<sub>2</sub> NPs were only occasionally seen within the lysosome of A594 cells (Figure 8B). Vast majority of the laser Ag NPs is located outside the A594 cell membrane (Figure 8A). Previous finding by Xu et al<sup>42</sup> demonstrated that NPs located in the nuclei or ribosomes of the cells were more toxic than those in the cytoplasm, even at low concentrations. In our study, we did not observe any laser Ag-TiO<sub>2</sub> NPs that were in the nuclei. The lack of nuclear location of Ag-TiO<sub>2</sub> NPs, together with the nicely preserved structures of mitochondrial and

other organelles, suggest that the toxic effect of the laser Ag-TiO<sub>2</sub> NPs to human cells could be very mild.

One limitation of the current study is that, the cytotoxicity experiment was only conducted for up to 72 hours on the in vitro cell culture model. In vivo experiment on animal models will be useful to evaluate the long-term accumulation of the laser-generated Ag-TiO<sub>2</sub> NP. Further studies could also separate NPs into different sizes using fractionation techniques to more precisely determine their correlation of the Ag-TiO<sub>2</sub> NPs size with the biological function and toxicity.

## Conclusion

The picoseconds laser-generated Ag-TiO<sub>2</sub> compound NPs demonstrated strong antibacterial activity against 3 types of bacteria (*E. coli*, *P. aeruginosa*, *S. aureus*), including the methicillin-resistant strain, MRSA, under standard laboratory daylight condition. The mechanisms contributing to the antibacterial properties were found to be ROS generation, GSH reduction, LPO, cell membrane damages and protein leakage. Up to 3 days co-culture, the laser-generated Ag-TiO<sub>2</sub> NPs showed low toxicity to the human cells originated from the lung, kidney, liver, skin and blood vessel cells. The laser-generated Ag-TiO<sub>2</sub> NPs mostly attached themselves to the human cell plasma membranes and few penetrated into the cells and none was found in the cell nucleus. The antimicrobial properties of the new type of picoseconds laser-generated Ag-TiO<sub>2</sub> compound NPs could have potential biomedical applications.

## Acknowledgments

The authors would like to thank Mr Abubaker Hamad from the School of Mechanical, Aerospace and Civil Engineering, the University of Manchester for his assistance in the generation of Ag NPs using laser ablation technology.

## Disclosure

The authors report no conflicts of interest in this work.

## References

- Rai M, Yadav A, Gade A. Silver nanoparticles as a new generation of antimicrobials. *Biotechnol Adv*. 2009;27(1):76–83.
- Avalos A, Haza AI, Mateo D, Morales P. Interactions of manufactured silver nanoparticles of different sizes with normal human dermal fibroblasts. *Intl Wound J*. 2016;13(1):101–109.
- Aditya NP, Vathsala PG, Vieira V, Murthy RS, Souto EB. Advances in nanomedicines for malaria treatment. *Adv Colloid Interface Sci*. 2013; 201–202:1–17.
- Juan L, Zhimin Z, Anchun M, Lei L, Jingchao Z. Deposition of silver nanoparticles on titanium surface for antibacterial effect. *Int J Nano-medicine*. 2010;5:261–267.
- Yu B, Leung KM, Guo Q, Lau WM, Yang J. Synthesis of Ag–TiO<sub>2</sub> composite nano thin film for antimicrobial application. *Nanotechnology*. 2011;22(11):115603.
- Gupta K, Singh R, Pandey A, Pandey A. Photocatalytic antibacterial performance of TiO<sub>2</sub> and Ag-doped TiO<sub>2</sub> against *S. aureus*, *P. aeruginosa* and *E. coli*. *Beilstein J Nanotechnol*. 2013;4(1):345–351.
- Ramesh P, Muthukumarasamy S, Dhanabalan K, Sadhasivam T, Gurunathan K. Synthesis and characterization of Ag and TiO<sub>2</sub> nanoparticles and their anti-microbial activities. *Dig J Nanomater Biostruct*. 2012;7(4):1501–1508.
- Arabatzi I, Stergiopoulos T, Bernard M, Labou D, Neophytides S, Falaras P. Silver-modified titanium dioxide thin films for efficient photodegradation of methyl orange. *Appl Catal B Environ*. 2003;42(2): 187–201.
- Ashkarran A. Antibacterial properties of silver-doped TiO<sub>2</sub> nanoparticles under solar simulated light. *J Theoret Appl Phys*. 2011;4(4): 1–8.
- Korshed P, Li L, Liu Z, Wang T. The molecular mechanisms of the antibacterial effect of picosecond laser generated silver nanoparticles and their toxicity to human cells. *PLoS One*. 2016;11(8):e0160078.
- Hajipour MJ, Fromm KM, Ashkarran AA, et al. Antibacterial properties of nanoparticles. *Trends Biotechnol*. 2012;30(10):499–511.
- Mills A, Le Hunte S. An overview of semiconductor photocatalysis. *J Photochem Photobiol*. 1997;108(1):1–35.
- Shukla RK, Sharma V, Pandey AK, Singh S, Sultana S, Dhawan A. ROS-mediated genotoxicity induced by titanium dioxide nanoparticles in human epidermal cells. *Toxicol In Vitro*. 2011;25(1):231–241.
- Biello D [webpage on the Internet]. Do nanoparticles and sunscreen mix? *Scient Am*. Available from: <http://www.scientificamerican.com/article.cfm?id=do-nanoparticles-and-sunscreen-mix>. 2007. Accessed September 1, 2016.
- Drake PL, Hazelwood KJ. Exposure-related health effects of silver and silver compounds: a review. *Ann Occup Hyg*. 2005;49(7):575–585.
- Bartłomiejczyk T, Lankoff A, Kruszewski M, Szumiel I. Silver nanoparticles allies or adversaries? *Ann Agric Environ Med*. 2013;20(1):48–54.
- Liu W, Wu Y, Wang C, et al. Impact of silver nanoparticles on human cells: effect of particle size. *Nanotoxicology*. 2010;4(3):319–330.
- Liu X, Liu Z, Lu J, Wu X, Chu W. Silver sulfide nanoparticles sensitized titanium dioxide nanotube arrays synthesized by in situ sulfurization for photocatalytic hydrogen production. *J Colloid Interface Sci*. 2014;413:17–23.
- Jhuang YY, Cheng WT. Fabrication and characterization of silver/titanium dioxide composite nanoparticles in ethylene glycol with alkaline solution through sonochemical process. *Ultrason Sonochem*. 2016;28:327–333.
- Massa MA, Covarrubias C, Bittner M, et al. Synthesis of new antibacterial composite coating for titanium based on highly ordered nanoporous silica and silver nanoparticles. *Mater Sci Eng C Master Biol Appl*. 2014; 45:146–153.
- Pan X, Medina-Ramirez I, Mernaugh R, Liu J. Nanocharacterization and bactericidal performance of silver modified titania photocatalyst. *Colloids Surf B Biointerfaces*. 2010;77(1):82–89.
- Hamad A, Li L, Liu Z, Zhong XL, Liu H, Wang T. Generation of silver titania nanoparticles from an Ag–Ti alloy via picosecond laser ablation and their antibacterial activities. *RSC Advances*. 2015;5(89): 72981–72994.
- Hamad A, Li L, Liu Z. A comparison of the characteristics of nanosecond, picosecond and femtosecond lasers generated Ag, TiO<sub>2</sub> and Au nanoparticles in deionised water. *Appl Phys A*. 2015;120(4):1247–1260.
- Kavita K, Singh VK, Jha B. 24-Branched Δ<sup>5</sup> sterols from *laurencia papillosa* red seaweed with antibacterial activity against human pathogenic bacteria. *Microbiol Res*. 2014;169(4):301–306.
- Chhibber S, Kaur T, Kaur S. Co-therapy using lytic bacteriophage and linezolid: effective treatment in eliminating methicillin resistant *Staphylococcus aureus* (MRSA) from diabetic foot infections. *PLoS One*. 2013;8(2):e56022.

26. Xu H, Qu F, Xu H, et al. Role of reactive oxygen species in the antibacterial mechanism of silver nanoparticles on *Escherichia coli* O157: H7. *Biometals*. 2012;25(1):45–53.
27. Wang T, Holt CM, Xu C, et al. Notch3 activation modulates cell growth behaviour and cross-talk to Wnt/TCF signalling pathway. *Cell Signal*. 2007;19(12):2458–2467.
28. Elliott GC, Gurtu R, McCollum C, Newman WG, Wang T. Foramen ovale closure is a process of endothelial-to-mesenchymal transition leading to fibrosis. *PLoS One*. 2014;9(9):e107175.
29. Kim SH, Lee HS, Ryu DS, Choi SJ, Lee DS. Antibacterial activity of silver-nanoparticles against *Staphylococcus aureus* and *Escherichia coli*. *Korean J Microbiol Biotechnol*. 2011;39(1):77–85.
30. Dhanalekshmi K, Meena K, Ramesh I. Synthesis and characterization of Ag@ TiO<sub>2</sub> core-shell nanoparticles and study of its antibacterial activity. *Int J Nanotechnol*. 2013;3(5):5–14.
31. Pelgrift RY, Friedman AJ. Nanotechnology as a therapeutic tool to combat microbial resistance. *Adv Drug Deliv Rev*. 2013;65(13–14):1803–1815.
32. Yang XH, Fu HT, Wong K, Jiang XC, Yu AB. Hybrid Ag@ TiO<sub>2</sub> core-shell nanostructures with highly enhanced photocatalytic performance. *Nanotechnology*. 2013;24(41):415601.
33. Tamiolakis I, Fountoulaki S, Vordos N, Lykakis IN, Armatas GS. Mesoporous Au–TiO<sub>2</sub> nanoparticle assemblies as efficient catalysts for the chemoselective reduction of nitro compounds. *J Mater Chem A*. 2013;1(45):14311–14319.
34. Sripriya J, Anandhakumar S, Achiraman S, Antony JJ, Siva D, Raichur AM. Laser receptive polyelectrolyte thin films doped with biosynthesized silver nanoparticles for antibacterial coatings and drug delivery applications. *Int J Pharm*. 2013;457(1):206–213.
35. Fujishima A, Zhang X. Titanium dioxide photocatalysis: present situation and future approaches. *C R Chim*. 2006;9(5):750–760.
36. Cao H, Qiao Y, Liu X, et al. Electron storage mediated dark antibacterial action of bound silver nanoparticles: smaller is not always better. *Acta Biomater*. 2013;9(2):5100–5110.
37. Feinendegen LE. Reactive oxygen species in cell responses to toxic agents. *Hum Exp Toxicol*. 2002;21(2):85–90.
38. Huang Z, Maness P, Blake D, Wolfrum E, Smolinski S, Jacoby W. Bactericidal mode of titanium dioxide photocatalysis. *J Photochem photobiol A*. 2000;130(2–3):163–170.
39. Shi J, Sun X, Lin Y, et al. Endothelial cell injury and dysfunction induced by silver nanoparticles through oxidative stress via IKK/NF-κB pathways. *Biomaterials*. 2014;35(24):6657–6666.
40. Lankoff A, Sandberg WJ, Wegierek-Ciuk A, et al. The effect of agglomeration state of silver and titanium dioxide nanoparticles on cellular response of HepG2, A549 and THP-1 cells. *Toxicol Lett*. 2012;208(3):197–213.
41. Jennifer M, Maciej W. Nanoparticle technology as a double-edged sword: cytotoxic, genotoxic and epigenetic effects on living cells. *J Biomater Nanobiotechnol*. 2013;4(1):53–63.
42. Xu P, Van Kirk EA, Zhan Y, Murdoch WJ, Radosz M, Shen Y. Targeted charge-reversal nanoparticles for nuclear drug delivery. *Angew Chem Int Ed Engl*. 2007;46(26):4999–5002.

### International Journal of Nanomedicine

### Publish your work in this journal

The International Journal of Nanomedicine is an international, peer-reviewed journal focusing on the application of nanotechnology in diagnostics, therapeutics, and drug delivery systems throughout the biomedical field. This journal is indexed on PubMed Central, MedLine, CAS, SciSearch®, Current Contents®/Clinical Medicine,

Submit your manuscript here: <http://www.dovepress.com/international-journal-of-nanomedicine-journal>

Dovepress

Journal Citation Reports/Science Edition, EMBase, Scopus and the Elsevier Bibliographic databases. The manuscript management system is completely online and includes a very quick and fair peer-review system, which is all easy to use. Visit <http://www.dovepress.com/testimonials.php> to read real quotes from published authors.